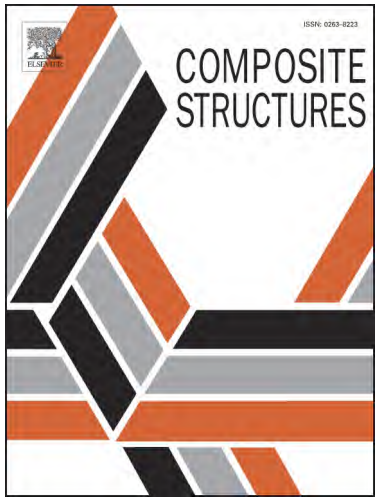

Optimization of Mechanical and Thermo-Mechanical Properties of Epoxy and E-Glass/Epoxy Composites Using NH_2-MWCNTs, Acetone Solvent and Combined Dispersion Methods

S. Zainuddin, A. Fahim, T. Arifin, M.V. Hosur, M.M. Rahman, J.D. Tyson, S. Jeelani

PII: S0263-8223(13)00590-4
DOI: http://dx.doi.org/10.1016/j.compstruct.2013.11.010
Reference: COST 5466

To appear in: *Composite Structures*

Please cite this article as: Zainuddin, S., Fahim, A., Arifin, T., Hosur, M.V., Rahman, M.M., Tyson, J.D., Jeelani, S., Optimization of Mechanical and Thermo-Mechanical Properties of Epoxy and E-Glass/Epoxy Composites Using NH_2-MWCNTs, Acetone Solvent and Combined Dispersion Methods, *Composite Structures* (2013), doi: http://dx.doi.org/10.1016/j.compstruct.2013.11.010

Optimization of Mechanical and Thermo-Mechanical Properties of Epoxy and E-Glass/Epoxy Composites Using NH_2-MWCNTs, Acetone Solvent and Combined Dispersion Methods

S. Zainuddin[a*], A. Fahim[a], T. Arifin[b], M. V. Hosur[a], M. M. Rahman[b], J.D. Tyson[b], S. Jeelani[a,b]

[a]*Department of Material Science and Engineering, Tuskegee University, Tuskegee, AL 36088*
[b]*Department of Mechanical Engineering, Tuskegee University, Tuskegee, AL 36088*

* Corresponding Author, e-mail: szainuddin@mytu.tuskegee.edu, Tel.: +1 334-724-4222, Fax: +1 334-724-4224

Abstract

We have used a combination of ultrasound processor and 3-roll shear mixer to disperse 0.2-0.4 wt. % functionalized multi-walled carbon nanotubes (MWCNTs- NH_2) in SC-15 epoxy with and without acetone media. Epoxy and e-glass/epoxy composites were prepared with this modified resin. In addition, control composites without MWCNT were also prepared for baseline comparison. Fourier transform infrared spectroscopy (FTIR), rheology, dynamic mechanical thermal analysis (DMTA) and flexure tests were conducted. Effective dispersion of MWCNTs achieved through solvent media, and the enhanced interfacial interaction between epoxy and amine functional groups of MWCNTs lead to optimum increase in DMTA and flexural properties of composites. Micrographic analyses revealed bridging of MWCNTs with epoxy and rougher fracture surfaces in epoxy composites. Also, a better interfacial bonding was observed in MWCNT incorporated e-glass/epoxy samples over control samples.

Keywords: Functionalized MWCNTs; Sonication; Calendaring; Acetone; Mechanical and thermo-mechanical properties

1. Introduction

Glass/epoxy composites are increasingly used in many structural applications replacing metallic materials due to their low cost, high strength, high chemical resistance and excellent insulating properties. However in most of these applications, fiber control the tensile load carrying capacity while compressive, bending, inter-laminar shear properties of composite structure depend on the properties of matrix [1]. In a fiber/matrix composite, matrix being the weakest component is first to fail upon such loading. Therefore, enhancement of matrix properties under such loading is desired to enhance the overall performance of fiber reinforced polymer (FRP) composites.

In recent years, researchers have successfully tailored the matrix properties by incorporating inorganic nanoparticles into epoxy polymer and its fiber-reinforced composites [2-5]. Among the nanoparticles, carbon nanotubes (CNTs) have emerged as potential candidates for modification of matrix because of its exceptional strength and stiffness, high flexibility, diameter dependent specific surface area and high aspect ratio. According to Reynaud et al. [6], an interface of 1 nm thick represents roughly 0.3% of the total volume of the polymers in micro particle filled composites, whereas it can reach 30% of the total volume in nanocomposites. The high specific surface area of CNTs provide desirable interface for stress transfer but can introduce strong attractive forces in between CNTs causing excessive agglomeration and produce unwanted stress concentrations which acted as a precursor to failure. However, multi-walled carbon nanotubes (MWCNTs) have an approximate specific surface area of $200 m^2/g$ or less which is lower than SWNTs due to their much larger diameter and multiple graphene walls and thus exhibit better dispersibility.

One of the most critical challenges in fabricating CNTs reinforced composites is the dispersion of CNTs itself because of their strong tendency to re-agglomerate. Kim et al. have reported that degree of CNTs dispersion into epoxy strongly affected the matrix-dominated mechanical properties [7]. Various methods to disperse nanotubes in polymer resins, such as stirring, sonication and high shear mixing have been reported in literature [8-10]. Some researchers found acetone or methonal solvents used in isolation or in combination with sonication effectively distribute the CNTs in epoxy matrices [11-12].

Also, the interfacial adhesion between the CNTs and polymer remains a critical issue. To have sufficient stress transfer from the matrix to the CNTs and to efficiently use the potential of CNTs as structural reinforcement, a strong interfacial adhesion between the CNTs and polymer is desired. The interfacial adhesion between CNTs and matrix was reported to improve by functionalizing the CNTs. Tailored amino, carboxyl or glycidyl groups enable covalent bonding between CNTs and epoxy resulting in improved interfacial bonding. The positive effects of functionalized CNTs on the mechanical properties are reported by various researchers [9, 13-14]. Kim et al. compared the effect of silane and acid treated CNTs in carbon/epoxy composites and found 15% and 10% enhancement in flexural strength and modulus [15]. Moniruzzaman et al. found an improvement of 10-15% in flexural properties with 0.05 wt. % single-walled nanotubes (SWNTs) [16].

While numerous studies are conducted in the last two decades on the CNT reinforced composites, effective dispersion of CNTs and its interfacial bonding with polymer still remains challenge. The realization of CNT incorporated epoxy resin and its composites can be achieved by resolving the following main issues

a. Optimizing the dispersion of CNTs up to the utmost possible extent to provide the maximum sites for CNT and epoxy interaction
b. Improving the interfacial adhesion between the epoxy and CNTs by identical functional groups that is critical for stress transfer
c. Further, improving the interfacial bonding of e-glass/epoxy composite by creating a three-way interaction of identical epoxy, CNT and e-glass functional groups

In this work, we have addressed the above issues by utilizing acetone solvent media, combination of sonication and calendaring techniques, and using the amine functionalized MWCNTs and amine based epoxy resin. In addition, epoxy silane sized woven e-glass was used to establish a three-way interlink between e-glass, epoxy and MWCNTs for improving the interfacial bonding them. To the best of our knowledge, such a comprehensive study is not yet been reported and thus carries a high scientific significance.

Rheological, 3-point bend and dynamic mechanical thermal analysis (DMTA) tests were performed on 0 to 0.4 wt. % loading samples to investigate the effect of functionalized MWCNTs on resin viscosity, flexural and thermo-mechanical properties. Fourier transform infrared spectroscopy (FTIR) analyses were performed to assure the complete removal of acetone from epoxy composites. Effect of combined acetone solvent media, high shear mixing and sonication techniques on MWCNTs dispersion in epoxy suspension was investigated and compared with conventionally prepared samples (without acetone solvent). Transmission electron microscope (TEM) was used to see the dispersion state of MWCNTs in epoxy. In addition, effect of interaction of MWCNTs with epoxide groups and fiber/matrix bonding were investigated using scanning electron microscope (SEM). All results were compared with control samples containing no MWCNTs.

2. Experimental

2.1. Materials

SC-15 epoxy used in this study was a two part cyclo-aliphatic amine resin (Part A: diglycidylether of bisphenol A, aliphatic diglycidyl and Part B: hardener). Multi-walled carbon nanotubes functionalized using amino groups (-NH_2) was purchased from Nanocyl Inc. Figure 1(A-B) shows the scanning electron micrographs of as received carbon nanotubes at different magnifications. High specific surface area and cotton-like entanglements caused the formation of agglomerates as reported by Reynaud et al. [6]. As reinforcement in composites, e-glass woven fabric with a density of 2.58 g/cm^3 and a single fiber diameter of 14-16 µm was procured from Fiber Glast Development Corporation. E-glass fibers were sized with 0.5 wt. % epoxy silanes to increase the compatibility and to have better adhesion between fibers and epoxy matrix.

2.2. Manufacturing process

2.2.1. Dispersion of MWCNT-NH_2 into epoxy resin

Dispersion of MWCNTs in epoxy was carried out using conventional (C-) and solvent(S-) based methods. From now on, these methods are referred as C- and S- methods respectively.

Conventional method (C-)

At first, MWCNT-NH_2 was mixed manually with epoxy resin part-A as per calculated weight ratio. The mixture was then sonicated at room temperature for 1 hour at 35% amplitude and 40 second on/ 20 second off cycle pulse mode. Sonication process induces elevated pressure and temperature in the system, thus the mixture was cooled down to room temperature in a cooling bath maintained at 5 ºC. To further improve the dispersion of MWCNTs, the sonicated mixture was then passed through three rollers. In this three roll process, roller 1 and 3 rotates in the same

direction, whereas the roller 2 placed in between rotates in the opposite direction thereby inducing high shearing in the mixture. A varying gap setting between the rolls and multiple passes of 20 µm (1st pass), 10 µm (2nd pass) and 5 µm (3rd pass) was used to induce high shear force in the mixture. The induction of high shear forces further de-agglomerates and improves the dispersion of CNTs in resin. Roller speed of the three rolls was maintained at a ratio of 1:3:9 with a maximum speed of 200 rpm was maintained in all the three passes.

Solvent method(S-)

At first, a calculated amount of MWCNTs was first added in 10 % by weight acetone of the total SC-15 epoxy resin. The mixture was than sonicated for 30 minutes at 20% amplitude followed by mixing with part-A for 1 hour using similar settings. Subsequently, this mixture was passed through the 3-rolls using similar conditions as of C- method. To ensure complete removal of acetone while maintaining uniform MWCNT dispersion, the mixture was heated to 70 °C on a magnetic stirrer maintained at a speed of 1000 rpm for 8 hours. The mixture weight was compared using a precise digital meter with the weight of mixture containing only SC-15+ MWCNT (conventionally prepared) after every hour.

Mixture prepared from both C- and S- methods was added individually in Part-B as per 10:3 stoichometric ratio and mixed with a high speed mechanical stirrer for 10 minutes at 800 rpm. The mixture was then placed in a desiccator for 30 minutes to remove the volatile impurities and entrapped air bubbles that were generated due to intense mechanical mixing. The mixture was then transferred into rectangular metal mold and cured for 4 hours at 60 °C and post-cured for 4 hours at 100 °C in a Lindberg/Blue Mechanical Convection Oven. Figure 2 shows the schematic of steps followed for fabrication in both methods.

2.2.2. Manufacturing of e-glass/epoxy nanocomposites

E-glass/epoxy nanocomposites were fabricated by using a combination of hand lay-up and compression hot press techniques. E-glass woven fabric layers were properly stacked into 7 plies and the orientation of fiber within the fabric was kept constant. Epoxy resin modified with MWCNTs was spread uniformly on each fabric layer and the laminate was consolidated by applying 133 kN force in a hot press. The temperature of hot press was maintained at 60 °C for 4 hours for curing followed by post curing in oven for 4 hours at 100 ºC. The final thickness of the panel was measured to be 3.2 mm.

2.3. Materials characterization

2.3.1. Rheology test

Rheology measurements were performed to observe the effect of increasing weight percent loading of MWCNTs on viscosity and the changes in viscosity as a measure of shear rate at constant temperature. Measurements were performed with AR 2000 Rheometer in ETC control mode using parallel plate geometry at 1000 µm gap settings. Flow sweep was used to vary the shear rate from 0.1 rad/sec to 100 rad/sec by keeping the temperature constant.

2.3.2. Fourier transform infrared spectroscopy (FTIR)

FTIR analyses were conducted on a Shimadzu FTIR 8400s instrument equipped with MiRacle TM ATR. Data were recorded at a resolution of 4 cm-1 from 650 to 3500 cm-1 with an averaging of 50 scans for removal of noise. The samples were analyzed from KBr pellets.

2.3.3. Thermo-mechanical Analysis

Dynamic mechanical thermal analysis (DMTA) was performed according to ASTM D4065-01 [17] to study the viscoelastic behavior of composite samples. It is also an effective way to

investigate the dispersion state of MWCNTs. In this test, the width of the samples was 12 mm and span length to thickness ratio was 10. Tests were conducted in dual cantilever beam mode with a frequency of 1 Hz and amplitude of 15 μm. The temperature was ramped from 30 to 130 ºC at a rate of 5 ºC/min. A minimum of three specimens of each type were tested. Storage modulus and glass transition temperature of samples were determined to evaluate the viscoelastic and damping properties of control and MWCNTs incorporated epoxy composites.

2.3.4. Mechanical testing

Three point bend flexure test was conducted according to ASTM D790-02 [18]. The dimension of epoxy samples was 75x12x4 mm (span length x width x thickness) and e-glass/epoxy samples was 52mm x 3.2mm x 12.2mm dimensions. A required span-length ratio of 16:1 was maintained and a minimum of six specimens of each set were tested. The test was performed using a Zwick-Roell Z 2.5 testing machine in displacement control mode with a crosshead speed of 1.2 mm/min.

2.3.5. Micrographic analysis

Dispersion state of MWCNTs in epoxy resin was investigated by transmission electron microscopy (TEM) using a Zeiss EM10 Transmission Electron Microscope operated at 60kV. The analysis of fracture surfaces was carried out using a JEOL JSM-6400 scanning electron microscope (SEM) at 5-10 kV accelerating voltage. Specimen surfaces were coated with a thin gold film to increase their conductance for SEM observation.

3. Results and Discussion

3.1. Rheological properties

Rheology measurements were performed immediately after the degasification of mixture. Figure 3 shows viscosity as a function of shear rate for control and 0.2-0.4 wt. % MWCNTs-NH_2 incorporated epoxy resin. With increasing shear rate, a shear thinning behavior was observed and a declining trend in shear viscosity was noticed in all samples. Consequently, at high shear rate, a Newtonian behavior was observed in all the samples independent of shear rate. Viscosity of 0.1 wt. % sample remained at comparable range with control resin. However, a rise in viscosity was observed with increasing weight percent of MWCNTs content. Viscosity of 0.4 wt. % resin samples was found to increase more than 100% in comparison to control samples. The multiple fold increase in shear viscosity with increasing CNT content has resulted due to strong particle-particle interaction of CNTs that may cause poor dispersion in epoxy matrix.

3.2. Fourier transform infrared spectroscopy (FTIR) analyses

The FTIR spectra provide information on the changes in molecular structure of samples through displacement, widening, appearance of bands. Figure 4 show the FTIR spectra of control and 0.2 wt. % samples in uncured conditions. It can be seen that the bands are quite similar, indicating that the use of acetone does not appear to change the chemical structure of epoxy, similar to as reported by Lau et al. [19]. It can be also be seen that the peak specifically related to acetone [20-21] at 1705-1730 cm^{-1} due to the stretching of C=O could not be identified separately as similar peaks was also found in uncured SC-15 epoxy resin. However, a distinct behavior of uncured and cured epoxy samples was found specifically in a band between 829-1035 cm^{-1} (Fig. 5). The peaks in this band disappeared in both control and 0.2 wt. % samples

cured after the removal of acetone. In addition, the peak at 1729 cm^{-1} shown in Fig. 4 was also disappeared in these samples. On the other hand, these peaks were still remained in samples cured without the removal of acetone. The disappearance of peaks in samples cured after the removal of acetone clearly indicates that the acetone was evaporated completely which otherwise can significantly affect the crosslinking and can decrease the conversion degree of reactive groups [19, 22].

3.3. Viscoelastic/ Thermo-mechanical properties of epoxy nanocomposites

Figure 6-7 show the storage modulus and glass transition temperature (T_g) vs. temperature response of all the samples obtained from DMTA test. Storage modulus of MWCNTs incorporated samples was relatively higher in both glassy and rubbery regions in comparison to control samples irrespective of the manufacturing process. Similarly, the glass transition temperature (T_g) was also improved with increase in MWCNT weight percent loading as shown in Fig. 7. Specimens at 0.3 wt. % loading prepared using S- method showed optimum increase of 72 % and 24 °C in storage modulus and T_g in comparison to control counterpart.

Better dispersion of MWCNTs at 0.3 wt. % evident from Fig. 8A provided more sites for MWCNT/polymer interaction, whereas, the presence of amino functional groups of MWCNTs reacted with epoxy forming a strong covalent bond as shown in Fig. 9 [23]. Samples fabricated using the S- method may have further assisted in the dispersion and interaction of MWCNTs with epoxy monomers. Dispersion of MWCNTs in acetone using the ultrasound processor may have de-agglomerated the tubes prior to mixing with part-A of SC-15 epoxy. In addition, acetone solvent diluted the epoxy resin and reduced its viscosity thereby enhancing the efficiency of

MWCNTs dispersion in S- method samples. The improved interaction and formation of covalent bond may have reduced the epoxy chain molecular motion around nanotubes resulting in a strong shift of elastic, viscous and T_g properties in MWCNTs incorporated nanocomposites. However at 0.4 wt. % loading, a decrease in storage modulus was observed relative to 0.2-0.3 wt. % samples which can be attributed to increase of density and incapability of MWCNTs de-agglomeration evident from Fig. 8B leading to reduction in crosslinking sites. As a result, the molecular motion and movement of chain may have increased, that resulted in decrease of viscoelastic properties. However, use of acetone solvent at 0.4 wt. % loading has increased the dispersion (Fig. 8C) and provided more interaction sites, thus resulted in slight improvement in viscoelastic properties of S- samples in comparison to C- counterpart at similar loading evident from Figs. 6-7.

One obvious factor for improving thermo-mechanical properties is the formation of covalent bond between epoxy and nanotubes. In case of control epoxy sample, hydrogen atoms in amine groups of DETA molecule (hardener) react with the epoxide group of DGEBA resin molecules and forms self-crosslink with each other. As shown in Fig. 9, in case of nanophased samples, after mixing SC-15 epoxy part-A and MWCNT-NH_2, the interfacial reaction at first takes place between amine functional groups of MWCNTs and epoxide groups of DGEBA resin by ring opening reaction. This upon further mixing with part-B of epoxy resin establishes a strong covalent bond between epoxy and MWCNTs, and thereby increases the crosslinking sites and improves the interfacial bonding.

3.4. Flexural properties

3.4.1. Epoxy nanocomposites

Figure 10 and Table 1 show the typical stress-strain curve and variation in flexural properties of epoxy samples. A linear stress-strain behavior was observed in all the samples before the stress level reached its maximum value. All the samples imparted brittle failure indicated by a sudden drop in the peak stress shown in Fig. 10. The flexural properties were increased in 0.2-0.3 wt. % MWCNT samples irrespective of the manufacturing method. These enhancements in flexural properties correlated well with the thermo-mechanical results described in section 3.3. Flexural strength and modulus of 0.2-0.3 wt. % C- samples were improved by 24-24.5% and 11-12%, respectively. The optimum enhancement in these properties was observed in 0.3 wt. % S- samples with an increase of 42.2% and 20.4% increase in flexural strength and modulus. In contrast, these properties were decreased at 0.4 wt. % loading relative to 0.2-0.3 wt. % samples irrespective of manufacturing method shown in Table 1. However, it can be seen that the 0.4 wt. % S- samples showed 5-8% increase in flexural properties in comparison to C- samples at similar weight percent loading. Even though, this improvement in flexural properties of 0.4 wt. % S- method samples was lower than 0.2-0.3 wt. % samples, increase over C- samples at similar weight percent loading can be attributed to the improved dispersion of CNTs assisted by acetone solvent media.

Figure 11 (A-E) show the scanning electron micrographs (SEM) of control and 0.3-0.4 wt. % MWCNTs-NH_2 tested samples. Rougher fracture surfaces were observed in 0.3 wt. % samples indicating the high resistance offered by material to crack propagation. In contrast, the fracture surface of control and 0.4 wt. % C- samples was relatively smoother (Fig. 11A and D). The crack

in 0.4 wt. % samples was found to originate from a zone that appears to be a cluster of agglomerated MWCNTs (Fig. 11D). However, no such cluster was observed in 0.4 wt. % S- samples and the fractured surface showed a combination of smooth and rough regions indicating a mix-mode failure behavior (Fig. 11E).

Figure 12 (A-B) shows the optical micrographs of 0.3-0.4 wt. % fractured samples. As expected, in control and 0.2-0.3 wt. % samples irrespective of the manufacturing method used. The crack initiated from the tip where the point load was applied and propagated in the same direction leading to failure evident from Fig. 12A (indicated by dotted line). However, a distinct failure mode was noticed in 0.4 wt. % C- samples. As oppose to crack initiating from the tip of load applied, the crack was initiated from a zone that appears to be a cluster of several MWCNTs particles evident from Figs. 12B and 11D, respectively. Cluster of agglomerated CNTs in epoxy formed due to poor dispersion result in producing localized stress concentration zone in the system [24-26]. Thus, the crack initiated from this high stress concentrated zone in 0.4 wt. % C- samples that lead to premature failure.

Better dispersion and enhanced interfacial bonding increased the polymer chain rigidity and offered high resistance to crack propagation. As a result, flexural and thermo-mechanical properties of 0.2-0.3 wt. % samples improved significantly. On the other hand, a decrease in these properties at 0.4 wt. % loading can be attributed to strong attractive forces between MWCNTs leading to excessive agglomeration. Due to poor dispersion evident from Fig. 8B, MWCNTs remains in form of clusters in resin blends. Shear slippage of individual nanotubes within these clusters may occur [27]. Because of this, a reduction in load transfer capability between CNTs and matrix systems may have occurred resulting in decrease of properties at 0.4 wt. % loading. Hence, the flexural and thermo-mechanical properties were improved in small

loadings (0.2-0.3 wt. %). However, in case of 0.4 w% loading sample, uniform dispersion of CNTs into the matrix was found inefficient using the present dispersion technique. Moreover incorporation of higher weight percent loading increased the viscosity of matrix which may have impeded the dispersion [3]. Song et al. also performed rheological study and stated that poorly dispersed CNTs within epoxy have a higher viscosity than that of uniformly dispersed suspensions [28].

3.4.2. E-glass/epoxy nanocomposites

Figure 13 show the typical stress–strain behavior obtained from the 3-point bend tests. Summary of the flexural test results and variation in properties as a function of MWCNTs content are shown in Table 2. The flexural properties were found to improve significantly upto 0.3 wt. % loading in comparison to control counterpart. Flexural strength and strain to failure were improved with a maximum enhancement of 19% and 21.6 % in 0.3 wt. % S- samples in comparison to control samples. Also, the flexural strength was found maximum in 0.2 wt. % S- samples i.e. 23% higher in comparison to control samples. Similar to epoxy composite results (Table 1), no considerable differences in flexural properties of 0.2 and 0.3 wt. % samples were observed.

The enhancement in epoxy matrix properties due to the effective incorporation of MWCNTs directly translated in the improvement of 0.2-0.3 wt. % e-glass/epoxy samples flexural properties. Similar to the results described in previous sections, a decrease in flexural properties was observed at 0.4 wt. % MWCNTs loading. The high viscosity rise of epoxy resin due to high content and poor dispersion of CNTs may cause improper wetting of glass fibers during laminate fabrication that results in week fiber/matrix bonding [29]. This may have further added to the other factors described earlier that lead in decrease of flexural properties at 0.4 wt. % loading.

The increase in strain to failure of 0.2-0.3 wt. % e-glass/epoxy samples can be attributed to improved properties of epoxy matrix. Polymer matrix incorporated with amino-functionalized MWCNTs can increase the fracture energy as crack propagation can be resisted by bringing up the crack faces of nanotubes evident from Fig. 14[30]. Also, the crack propagation changes direction as it crosses CNTs during failure process due to bridging effect that prevents crack opening. As a result, crack initiation and propagation becomes difficult in the CNTs incorporated e-glass/epoxy samples.

Figure 15(A-C) shows the SEM micrographs of control and 0.3-0.4 wt. % (S-method) e-glass/epoxy samples failed in the direction of loading. The damage in 0.3 wt. % sample was found more intense in the vicinity of load applied with fibers were strongly bonded with the matrix shown in Fig. 15B. It is clearly evident from this figure, that the sample observed considerable energy before fracture. In contrast, poor fiber/matrix bonding was observed in control samples. As a result, crack propagated with less resistance as shown in Fig. 15A. However, in 0.4 wt. % samples, multiple cracks were found initiating at several locations that may have resulted in fiber/matrix delamination prior to actual failure shown in Fig. 15C.

Figure 16(A-F) shows the magnified SEM micrographs of fractured fibers of control and 0.3-0.4 wt. % S-method samples. As evident from these micrographs, the fiber in 0.3 wt. % sample contains considerable amount of epoxy resin residue and rougher fracture surface in comparison to control samples. Similarly, in 0.4 wt. % samples, distributed resin residue and rougher fracture surface were observed but not as profound as in 0.3 wt. % counterpart. In 0.4 wt. % S- samples, presence of mixed regions of dispersed and agglomerated MWCNTs exists. The interfacial bonding in well dispersed region may have improved the interfacial bonding whereas the agglomerated region contributed to the initiation of fracture. As a result, a distributed residue of

resin, rougher fracture surface (Fig. 16(E-F)) and several cracks (Fig. 15C) were observed in 0.4 wt. % sample. Thus, both the thermo-mechanical and flexural properties of 0.4 wt. % were found higher than control and lower than 0.3 wt. % samples, respectively.

Moreover, the presence of epoxy silane on the surface of e-glass fibers may have also reacted with amino groups of MWCNTs in addition to its reaction with epoxy matrix functional groups shown in Fig. 7. This improved three-way chemical reactivity lead to a strong covalent bonding that may have resisted the crack propagation and increased the fiber/matrix bonding in 0.2-0.3 wt. % MWCNTs samples. Thus, better dispersion and enhanced interfacial bonding between epoxy, MWCNTs and e-glass fibers lead to the improvement in thermo-mechanical and flexural properties of epoxy, and consequently of glass/epoxy composites.

4. Conclusion

In this work, functionalized MWCNTs were incorporated using combined mixing methods and acetone solvent media to enhance the flexural and viscoelastic properties of epoxy and e-glass/epoxy composites. Based on the experimental and micrographic results, the following conclusions are reached:

1. Dispersion of NH_2- MWCNTs using a combination of sonication and calendaring method, and acetone solvent increased viscoelastic and flexural properties at low concentrations of 0.2-0.3 wt. % loading.

2. Dynamic mechanical thermal analysis (DMTA) results of 0.3 wt. % S- samples showed a maximum improvement of 72% in storage modulus and an increase of 24 ºC in glass transition temperature in comparison to control samples.

3. Flexural test results of 0.3 wt. % samples prepared using S- method showed improvement in strength, modulus and strain to failure by 42%, 20% and 45% respectively in comparison to control samples.

4. Flexural test results of 0.3 wt. % samples prepared using S- method showed a maximum improvement in strength, modulus and strain to failure by 21%, 19% and 21.6% respectively in comparison to control samples.

5. Improvement at optimum loading of 0.3 wt. % explores a good interfacial interaction and effective load transfer between CNTs and epoxy system due to improved dispersion in presence of acetone solvent. Morphological studies have revealed that amino-functionalized MWCNTS promotes good adhesion between glass fiber and epoxy matrix by modifying the matrix adhesive properties and hence, the properties of composite increases.

6. Overall this work showed that amino-functionalized MWCNTs dispersed uniformly using the acetone solvent can significantly improve the mechanical and thermo-mechanical/viscoelastic properties of epoxy and its glass fiber reinforced composites.

Acknowledgements

The authors would like to acknowledge NASA-EPSCoR, NSF-EPSCoR and PREM, and DoD grants for funding this work.

References

1. Mallick PK. Fiber reinforced composites. New York: CRC press; 2007.
2. Farhana P, Zhou Y, Rangari V, Jeelani S. Testing and evaluation on the thermal and mechanical properties of carbon nano fiber reinforced SC-15 epoxy. Mater Sci Eng A 2005;405:246–53.
3. Gojny FH, Wichmann MHG, Fiedler B, Bauhofer W, Schulte K. Influence of nano modification on the mechanical and electrical properties of conventional fibre-reinforced composites. Compos Pt A: Appl Sci Manuf 2005;36(11):1525–35.
4. Mahfuz H, Adnan A, Rangari VK, Jeelani S, Jang BZ. Carbon nanoparticles/whiskers reinforced composites and their tensile response. Compos Part A: Appl Sci Manuf 2004;35:519–27.
5. Zhou Y, Farhana P, Lewis L, Jeelani S. Experimental study on the thermal and mechanical properties of multiwalled carbon nanotube-reinforced epoxy. Mater Sci Eng A 2007;452:657–64.
6. Reynaud E, Gauthier C, Perez J, Nanophases in polymer. Rev Metallurgy 1999;96:169–76.

7. Kim M, Park Y-B, Okoli O, Zhang C. Processing, characterization, and modeling of carbon nanotubes reinforced multiscale composites. Compos Sci Technol 2009;69:335–42.
8. Hassan M, Zainuddin S, Parker MR, Tariq A, Rangari VK, Jeelani S. Reinforcement of SC-15 epoxy with CNT/CNF under high magnetic field: an investigation of mechanical and thermal response. J Mater Sci 2009;44:1113-20.
9. Liao YH, Olivier MT, Liang ZY, Zhang C, Wang B. Investigation of the dispersion process of SWNTs/SC-15 epoxy resin nanocomposites; Mater Sci Eng A 2004;385:175–81.
10. Gojny FH, Nastalczyk J, Roslaniec Z, Schulte K. Surface modified multi-walled carbon nanotubes in CNT/epoxy-composites, Chem Phys Lett 2003;370:820-24.
11. Liao YH, Tondin OM, Liang Z, Zhang C, Wang B. Investigation of the dispersion process of SWNTs/SC-15 epoxy resin nanocomposites. Mater Sci Eng A 2004;385:175-181.
12. Domonteil S, Demortier A, Detriche S, Raes C, Fonseca A, Ruhle M, Nagy JB. Dispersion of carbon nanotubes using organic solvents. J. Nanosci and Nanotech 2006;6(5):1315-8.
13. Allaoui A, Bai S, Cheng HM, Bai JB. Mechanical and electrical properties of a MWNT/epoxy composite. Compos Sci Technol 2002;62:1993-8.
14. Bai J, Allaoui A. Effect of the length and aggregate size of MWNTs on the mechanical and electrical properties of the nanocomposites. Compos Part A 2003;34:689-94.
15. Kim MT, Rhee KY, Lee JH, Hui D, Lau A. Property enhancement of a carbon fiber/epoxy composite by using carbon nanotubes. Compos Part B 2011;42:1257-61.

16. Moniruzzaman M, Du F, Romero N, Winey K. Increased flexural modulus and strength in SWNT/epoxy composites by a new fabrication method. Polymer 2006;47:293-8.

17. Annual Book of ASTM Standards, D 4065-01, Standard Practice for Determining and Reporting Dynamic Mechanical Properties of Plastics, 2002.

18. Annual Book of ASTM Standards, D 790-02, Standard Test Methods for Flexural Properties of Unreinforced and Reinforced Plastics and Electrical Insulating Materials, 2002.

19. Lau KT, Lu M, Lam CK, Cheung HY, Sheng FL, Li HL. Thermal and mechanical properties of single-walled carbon nanotube bundle-reinforced epoxy nanocomposites: the role of solvent for nanotube dispersion. Compos Sci Technol 2005;65:719-25.

20. Max JJ, Chapados C. Infrared spectroscopy of acetone-hexane liquid mixtures. J Chm Phys 2007;126(15):154511.

21. Torii H, Musso M, Giorgini MG. Time-domain theoretical analysis of the noncoincidence effect, diagonal frequency shift, and the extent of delocalization of the C=O stretching mode of acetone/dimethyl sulfoxide binary liquid mixtures. J Phys Chem A 2005;109:7797.

22. Evtushenko YM, Ivanov VM, Zaitsev BE. Determination of epoxide and hydroxyl groups in epoxide resins by IR spectrometry. J Anal Chem 2003; 58(4):347-350.

23. Ma PC, Mo SY, Tang BZ, Kim JK. Dispersion, interfacial interaction and reagglomeration of functionalized carbon nanotubes in epoxy composites. Carbon 2010;48:1824–34.

24. Shokrieh MM, Saeedi A, Chitsazzadeh M. Mechanical properties of multi-walled carbon nanotube/polyester nanocomposites. JNanostruc Chem 2013;3:20.

25. Prashantha K, Soulestin J, Lacrampe MF, Krawczak P, Dupin G, Claes M. Masterbatch-based multi-walled carbon nanotube filled polypropylene nanocomposites: Assessment of rheological and mechanical properties. Compos Sci Technol 2009;69:1756-63.

26. Rahman MM, Zainuddin S, Hosur MV, Malone JE, Salam MBA, Kumar Ashok, Jeelani S. Improvements in mechanical and thermo-mechanical properties of e-glass/epoxy composites using amino functionalized MWCNTs. Compos Struc 2012;94:2397–2406

27. Dı´ez-Pascual A, Ashrafi B, Naffakh M, Gonza´ lez-Domı´nguez J, Johnston A, Simard B, Martı´nez M, Go´mez-Fatou M. Influence of carbon nanotubes on the thermal, electrical and mechanical properties of poly(ether ether ketone)/glass fiber laminates. Carbon 2011;49:2817-33.

28. Song YS, Yuon JR. Influence of dispersion states of carbon nanotubes on physical properties of epoxy nanocomposites. Carbon 2005;43:1378-85.

29. Hull D, Clyne TW. An introduction to composite materials. New York: Cambridge University Press; 1996.

30. Rahman M, Mahesh H., Zainuddin S, Uday V, Arifin T, A Kumar, Jonathan T, Jeelani S. Effects of amino-functionalized MWCNTs on ballistic impact performance of E-glass/epoxy composites using a spherical projectile. Inter J of Impact Engg 2013;57:108-118.

List of Figures

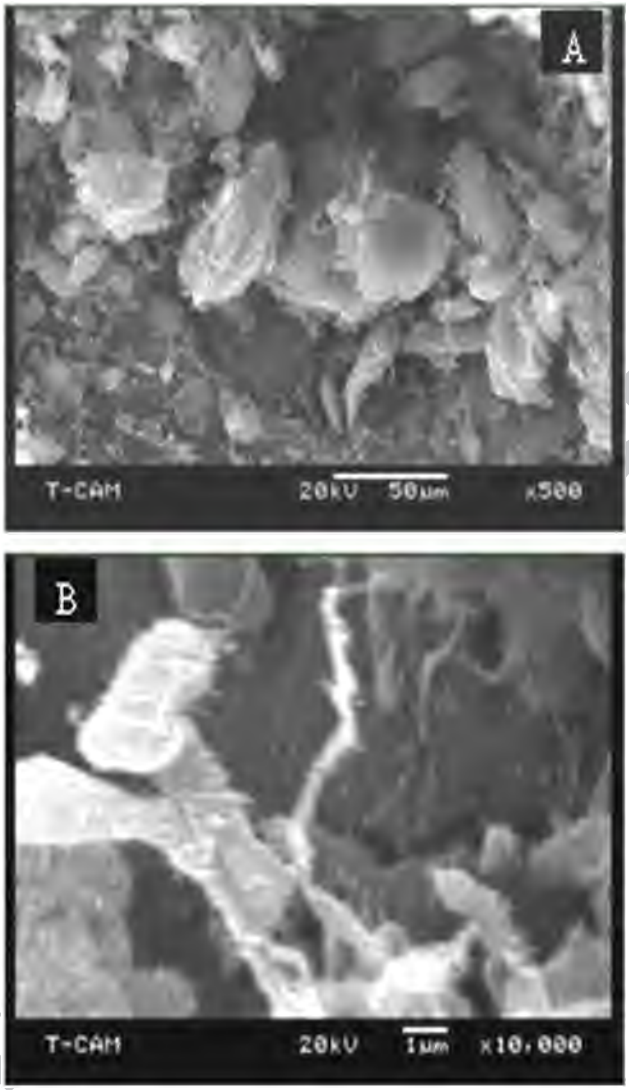

Figure 1(A-B). Scanning electron micrographs of as-received MWCNTs at magnification of 500x (A) and 10000x (B).

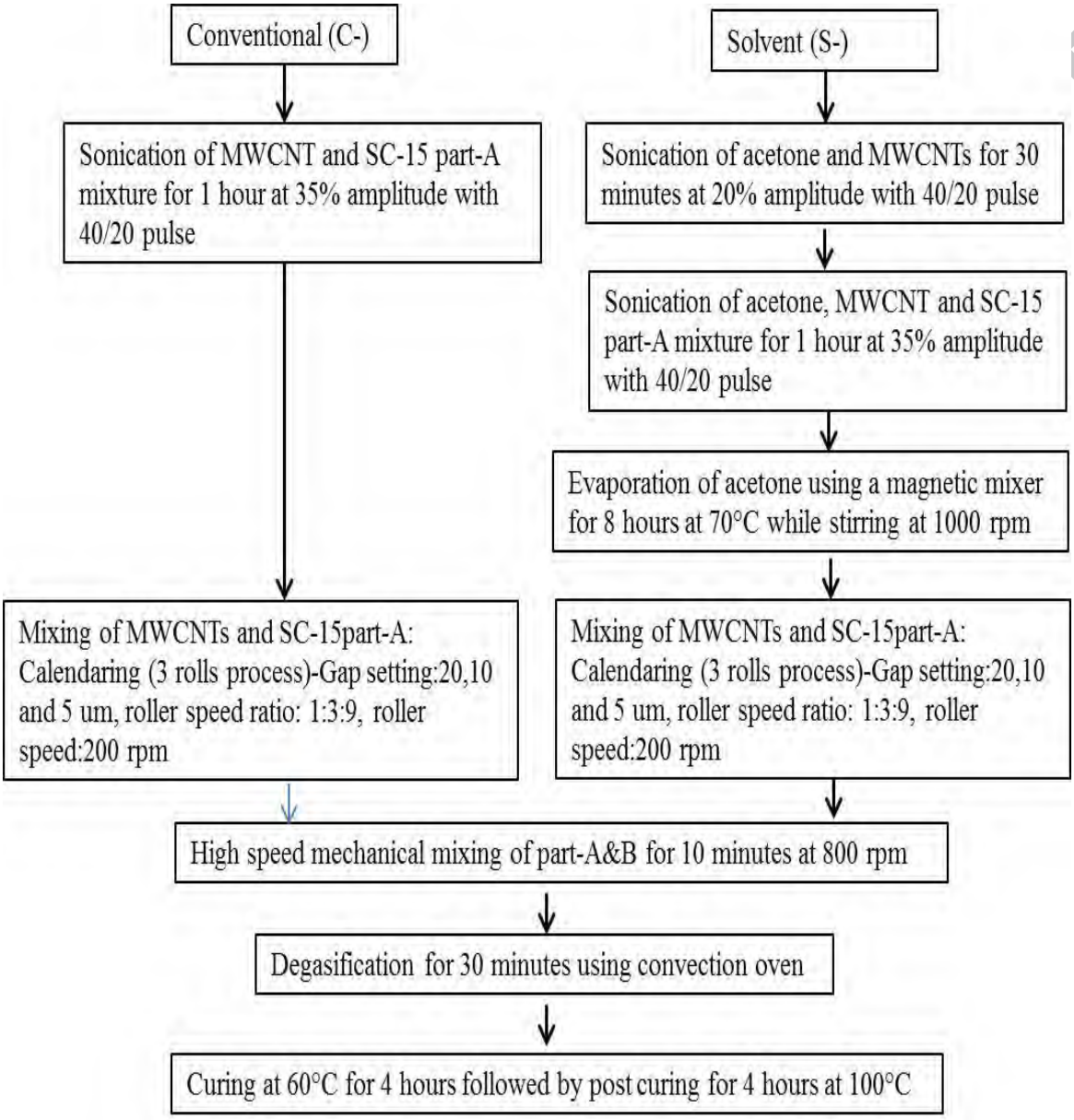

Figure 2. Schematic showing steps of MWCNTs reinforced epoxy composites fabrication using conventional (C-) and solvent (S-) method.

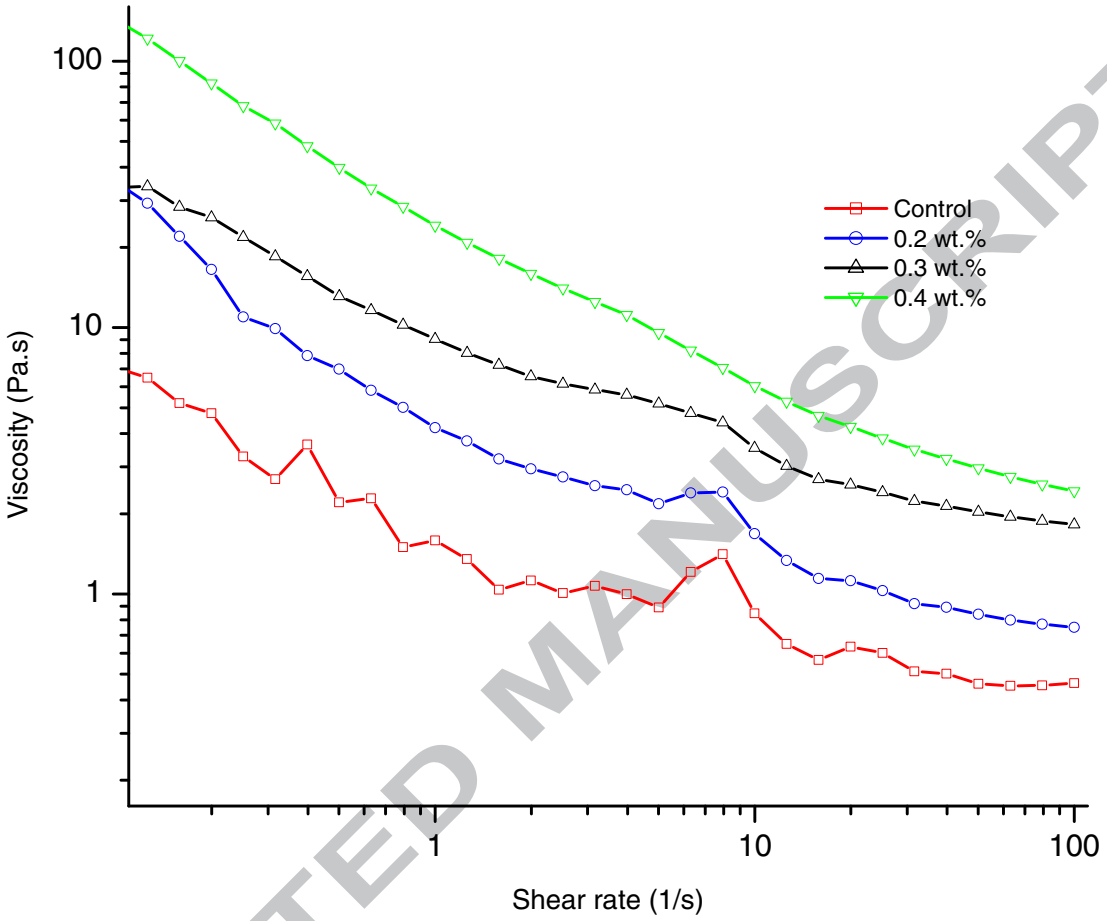

Figure 3. Viscosity vs. shear rate response of reference and MWCNTs-NH_2 incorporated epoxy resin.

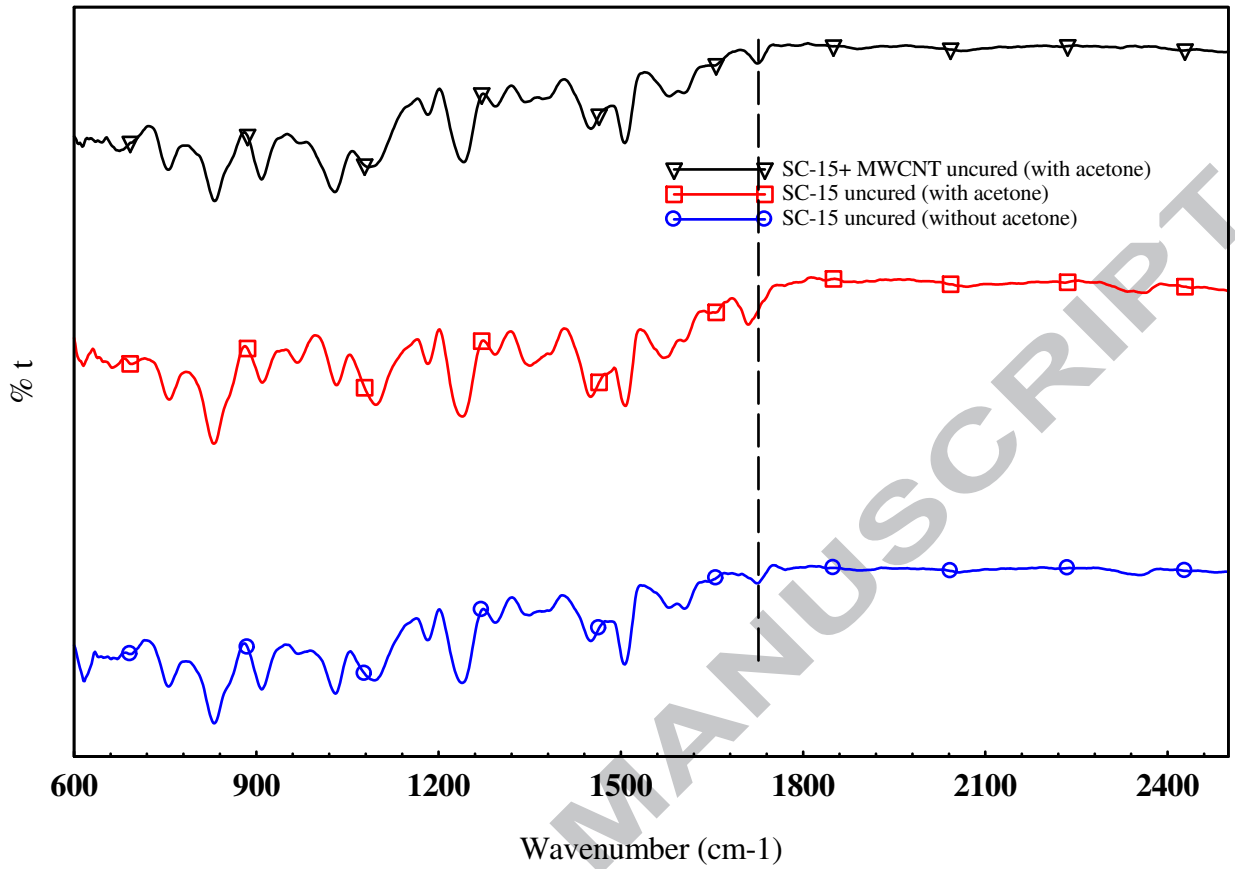

Figure 4. FTIR spectra of control and 0.2 wt. % MWCNT uncured epoxy samples.

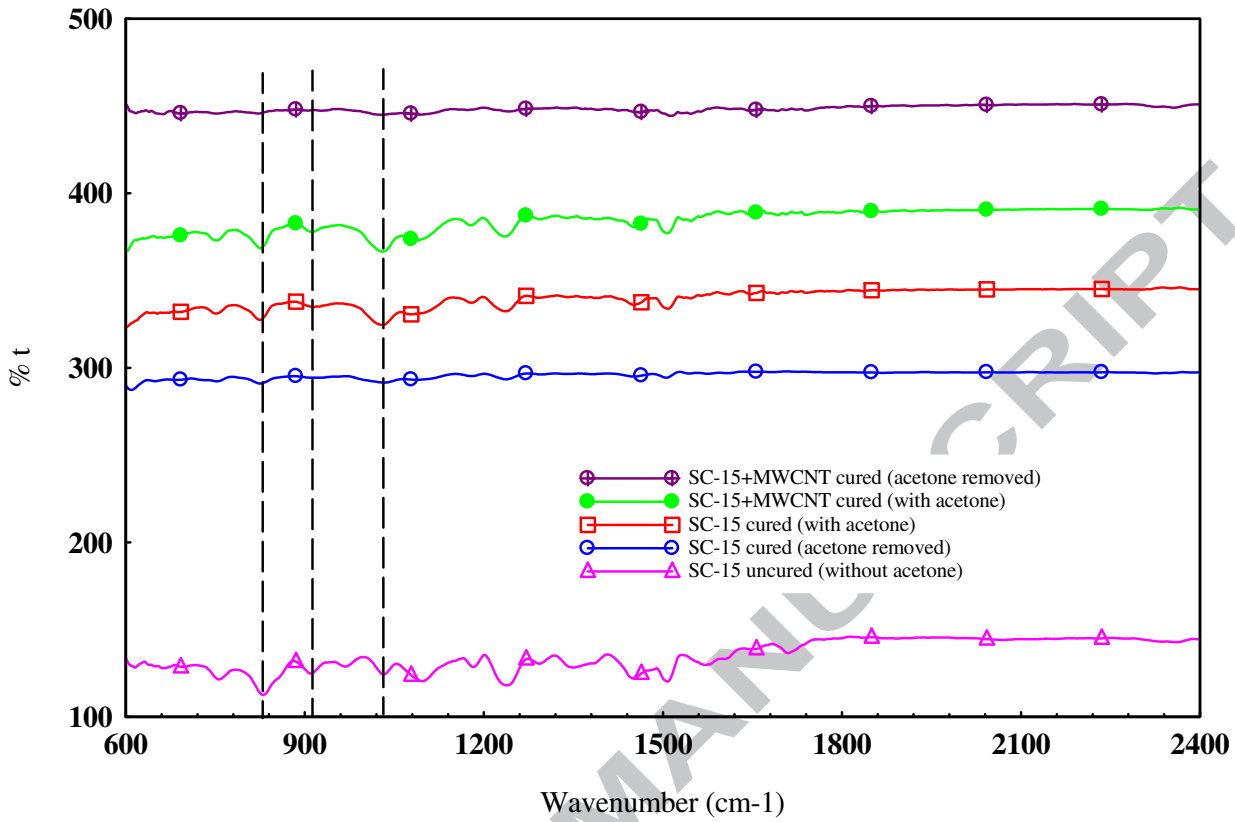

Figure 5. FTIR spectra of control and 0.2 wt. % MWCNT cured epoxy samples.

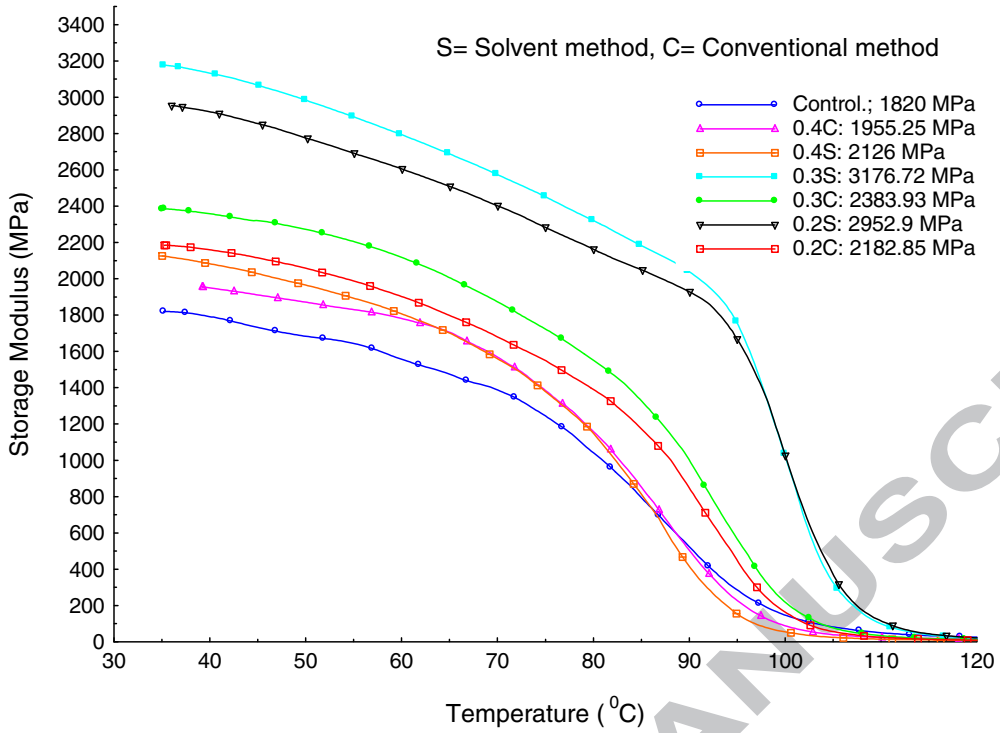

Figure 6. Storage modulus vs. temperature response of epoxy nanocomposites.

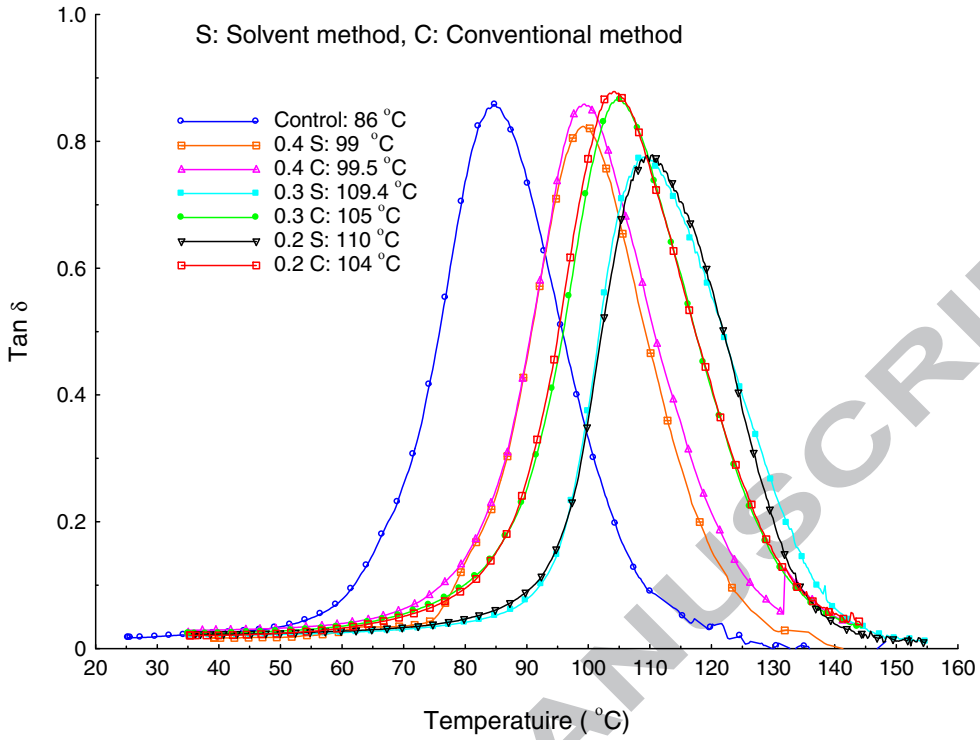

Figure 7. Tan delta vs. temperature response of e-glass/epoxy nanocomposites.

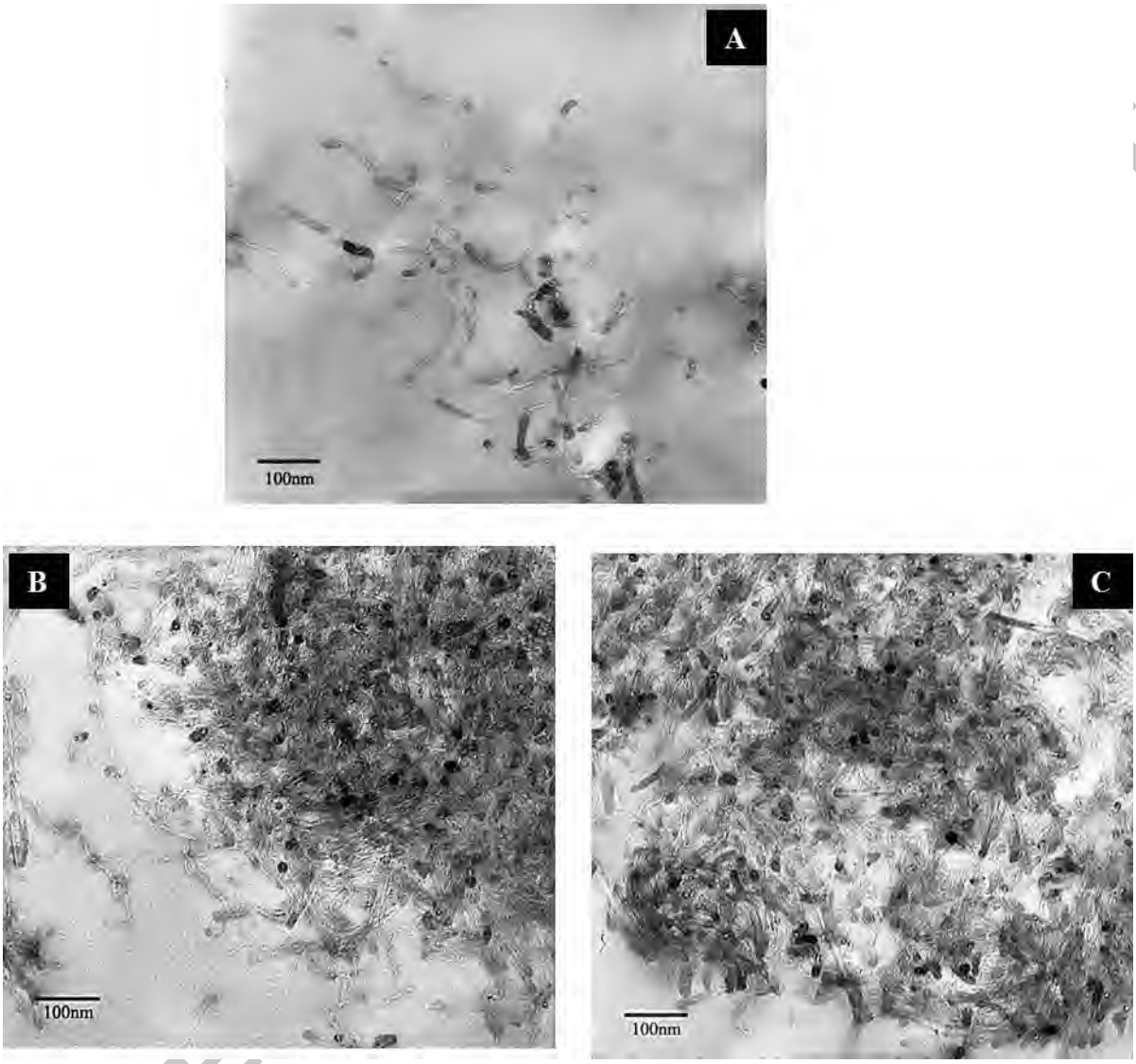

Figure 8 (A-C). Transmission electron micrographs of A) 0.3 wt. %, B) 0.4 wt. % conventional method, and C) 0.4 wt. % solvent method dispersed MWCNT-NH_2 in epoxy resin.

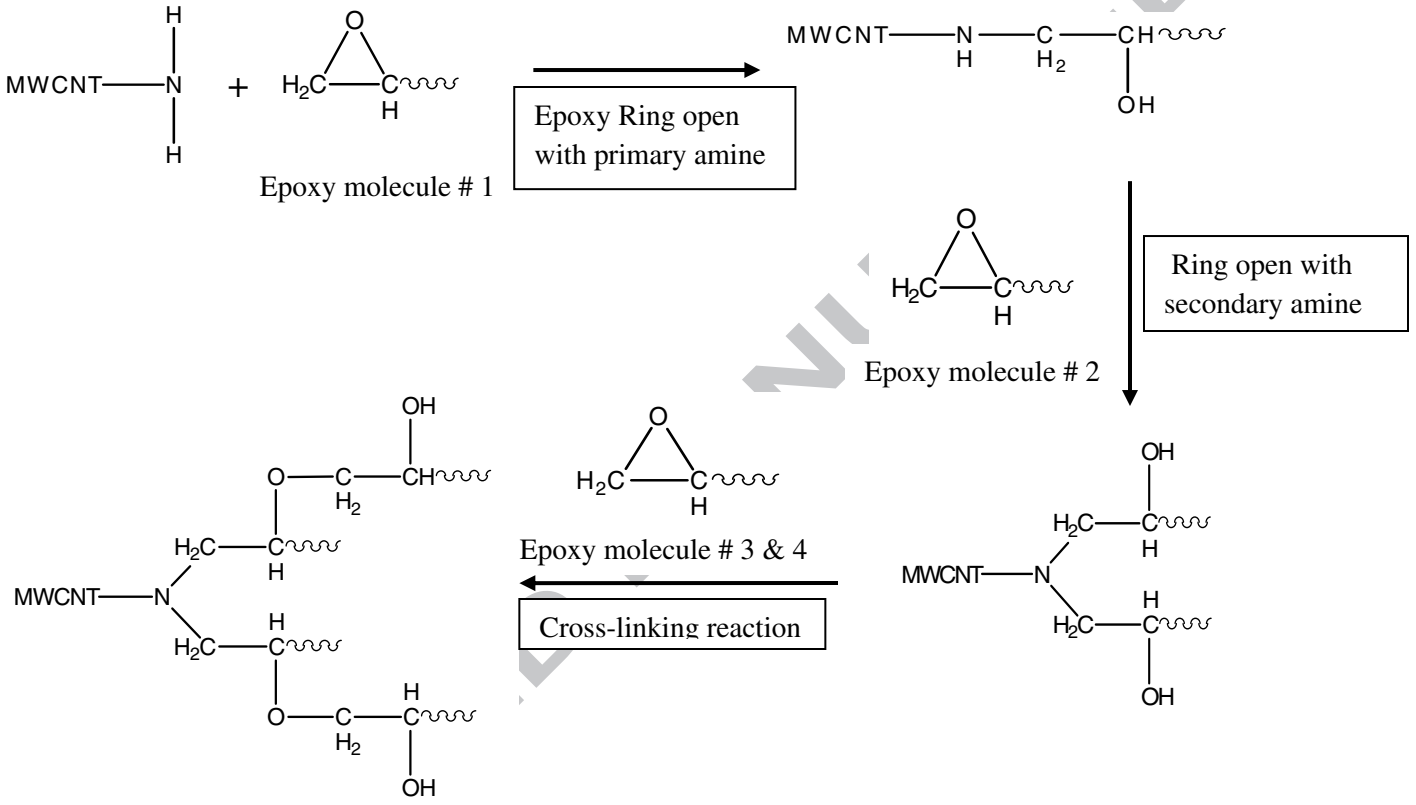

Figure 9. Schematic representation of interfacial reaction between DGEBA and MWCNT-NH_2.

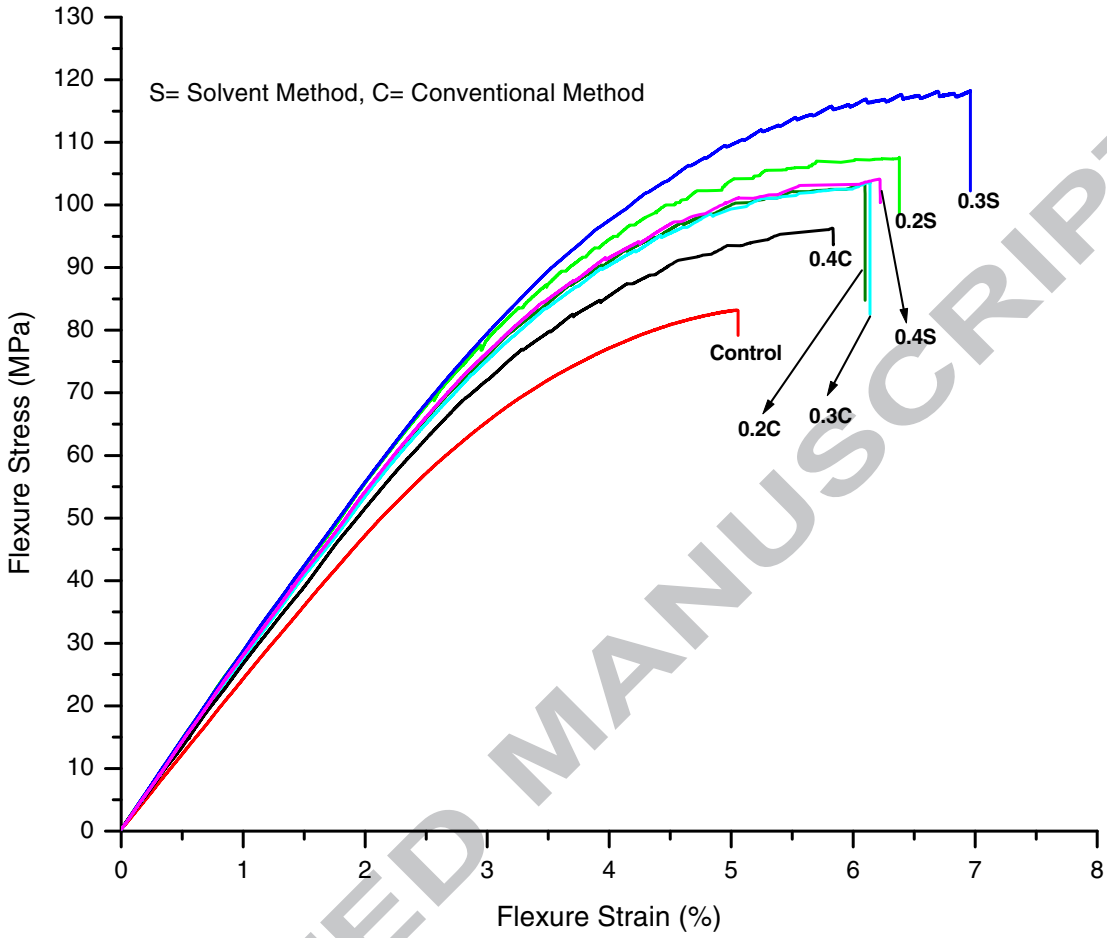

Figure 10. Flexural stress-strain response of control and MWCNTs-NH_2 incorporated epoxy composites.

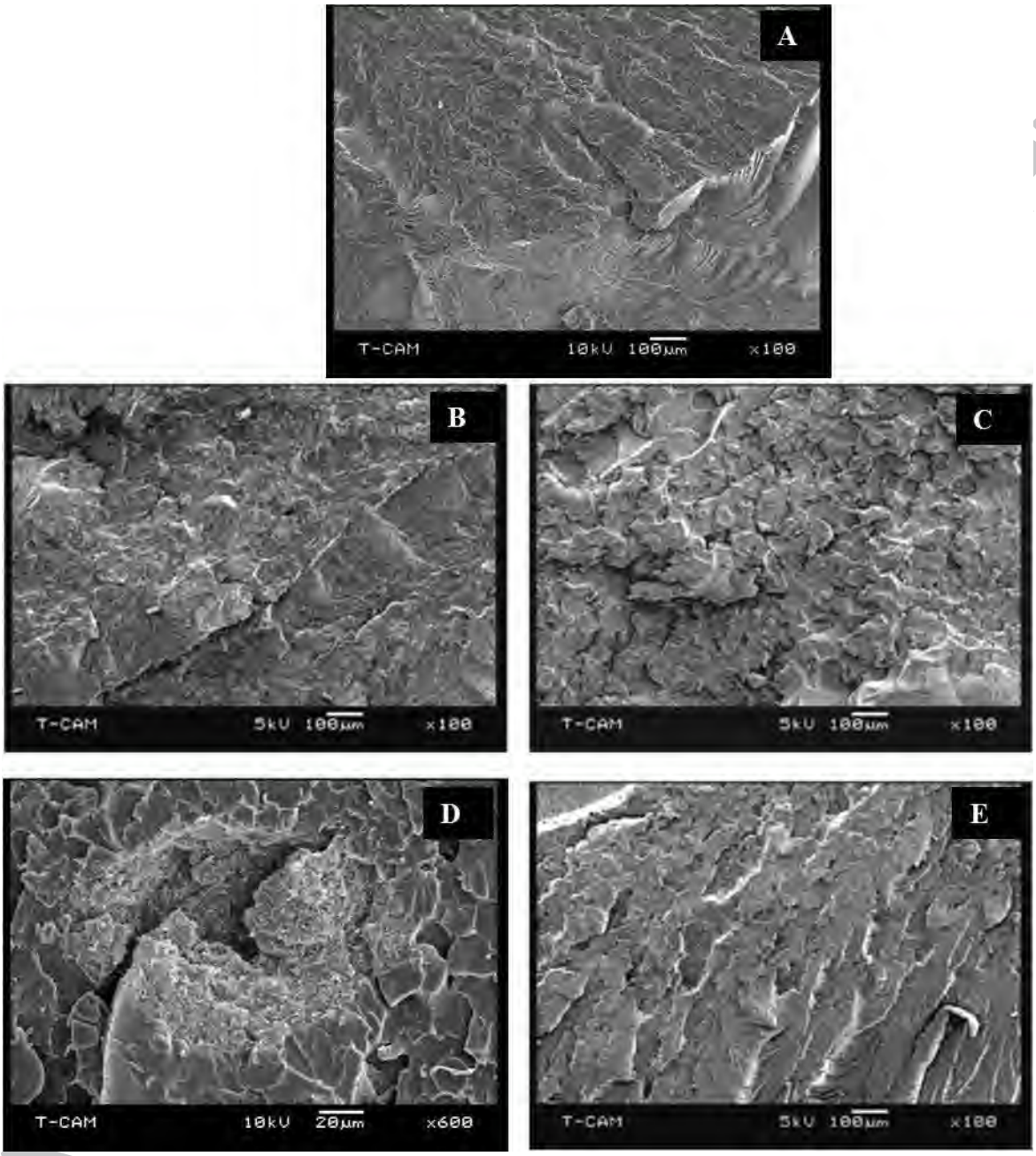

Figure 11(A-E). Fracture surfaces of A) control, B) 0.3C, C) 0.3S, D) 0.4C and, E) 0.4S of NH_2-MWCNTs epoxy samples.

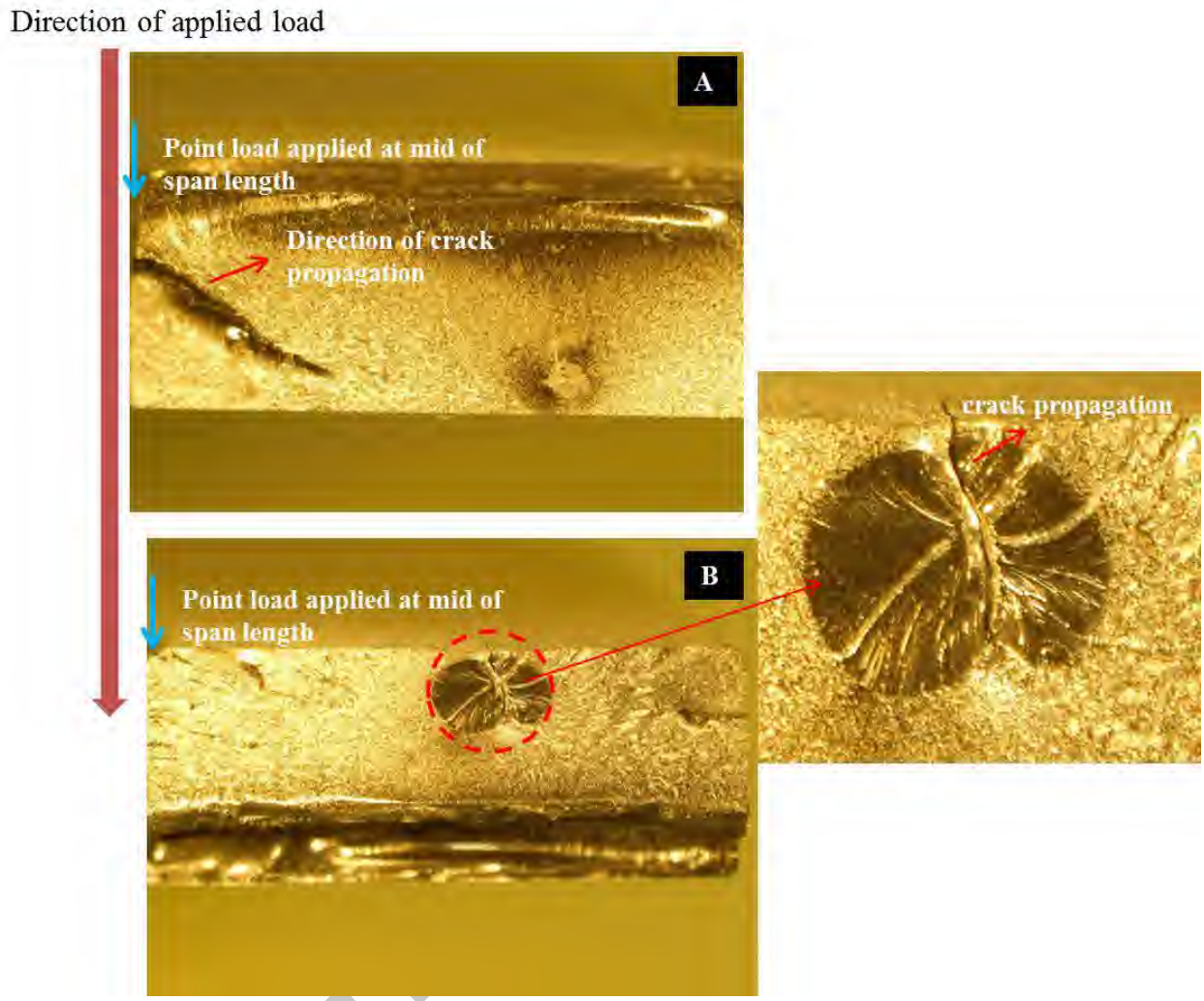

Figure 12 (A-B). Optical micrographs showing fracture in A) 0.3and, B) 0.4 wt. % MWCNTs-NH_2 epoxy samples.

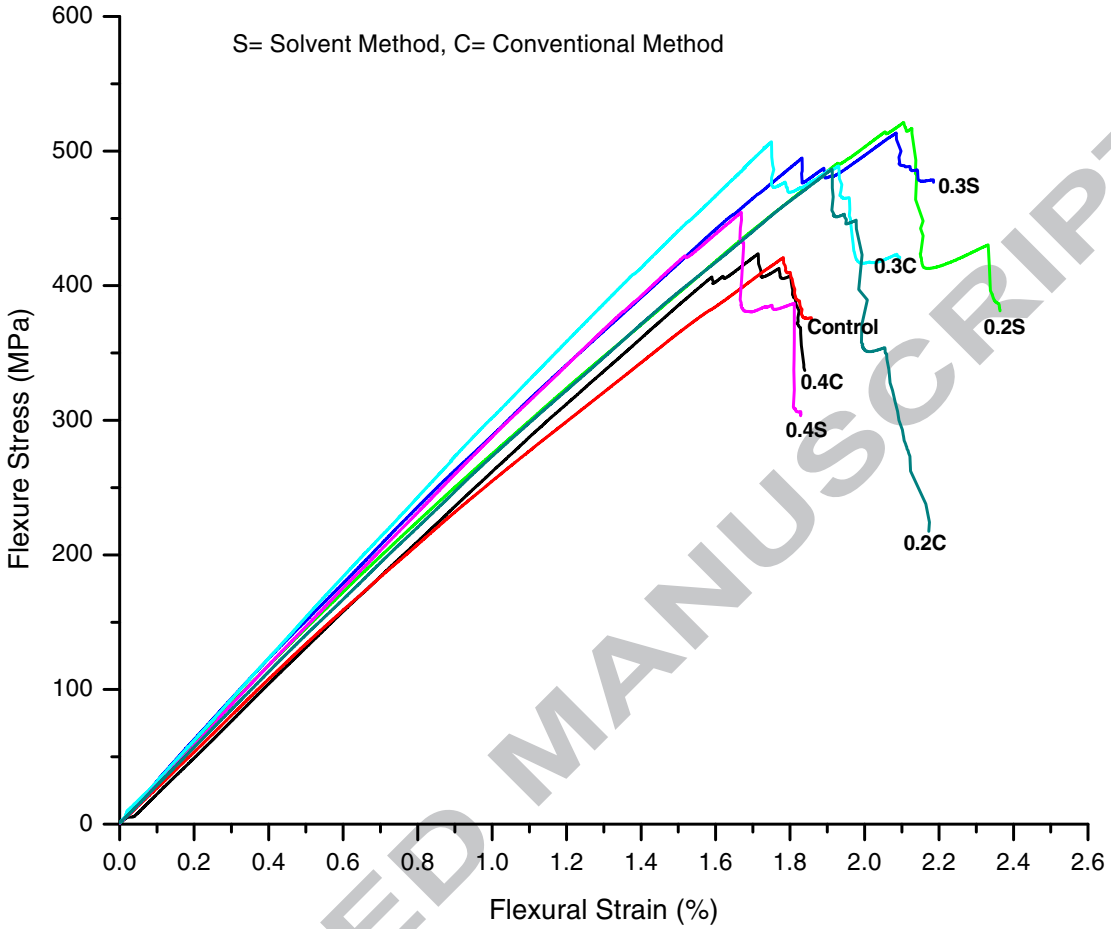

Figure 13. Flexural stress-strain response of control and MWCNTs-NH_2 incorporated e-glass/epoxy composites.

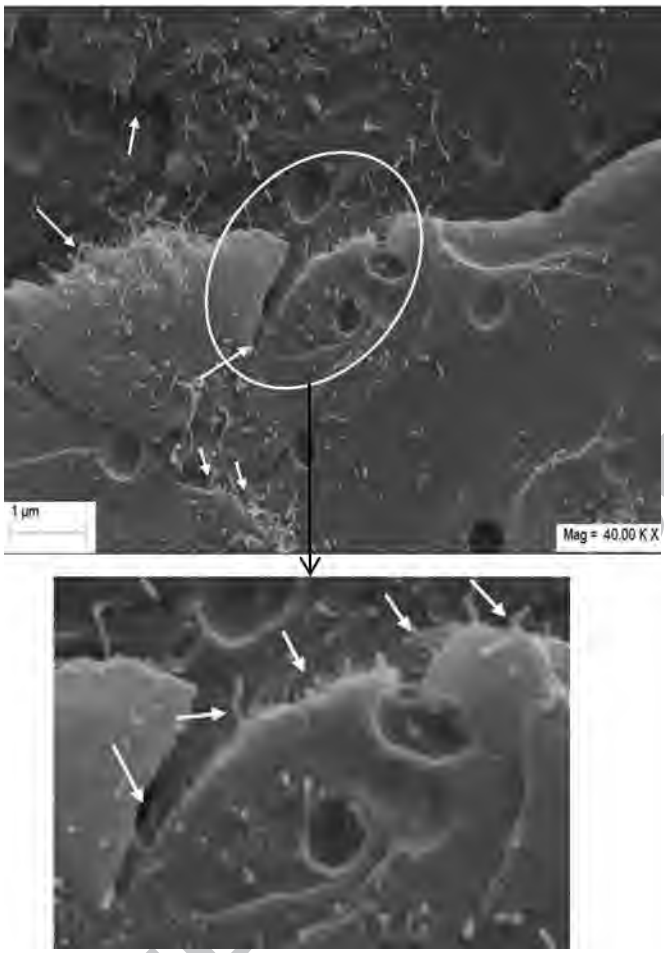

Figure 14. SEM Micrograph showing CNT pull-out and bridging between MWCNTs-NH_2 and epoxy resin.

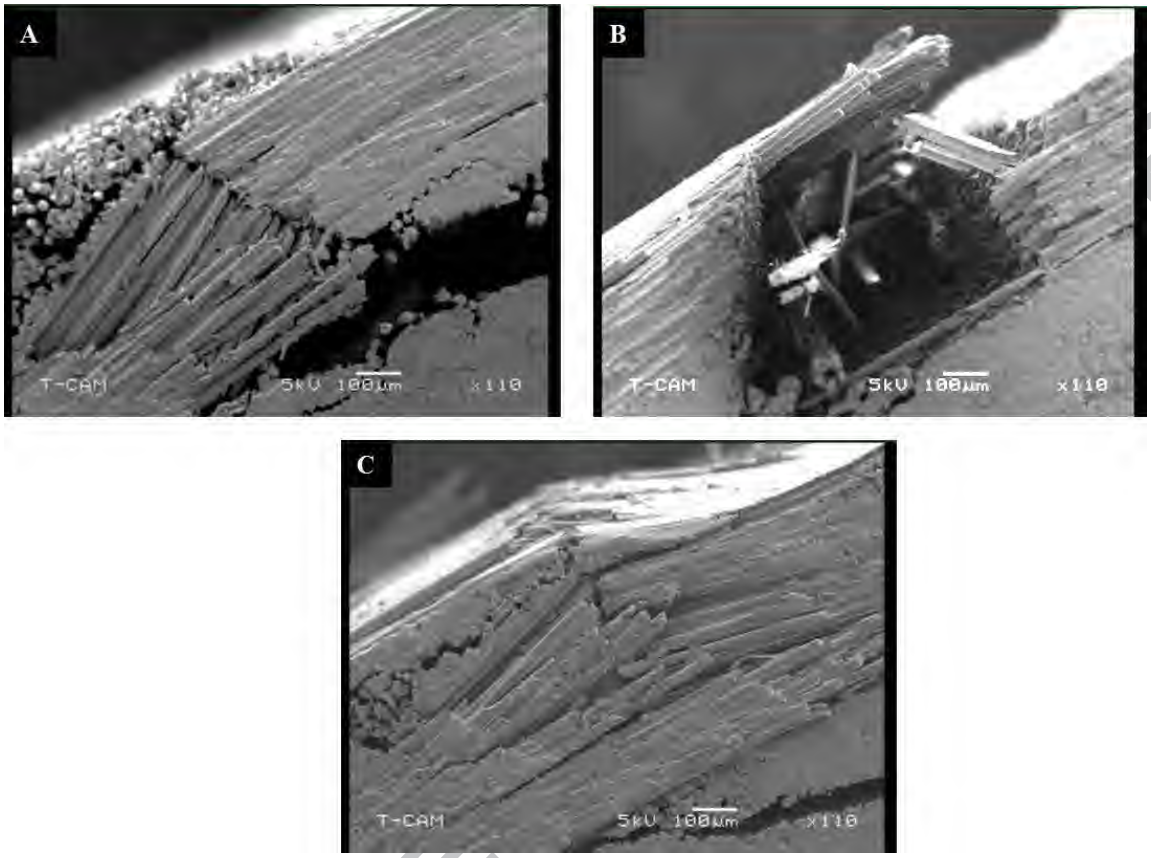

Figure 15 (A-C). SEM micrographs of fractured surface of A) control, B) 0.3 wt. % and, C) 0.4 wt. % MWCNTs incorporated e-glass/epoxy composites.

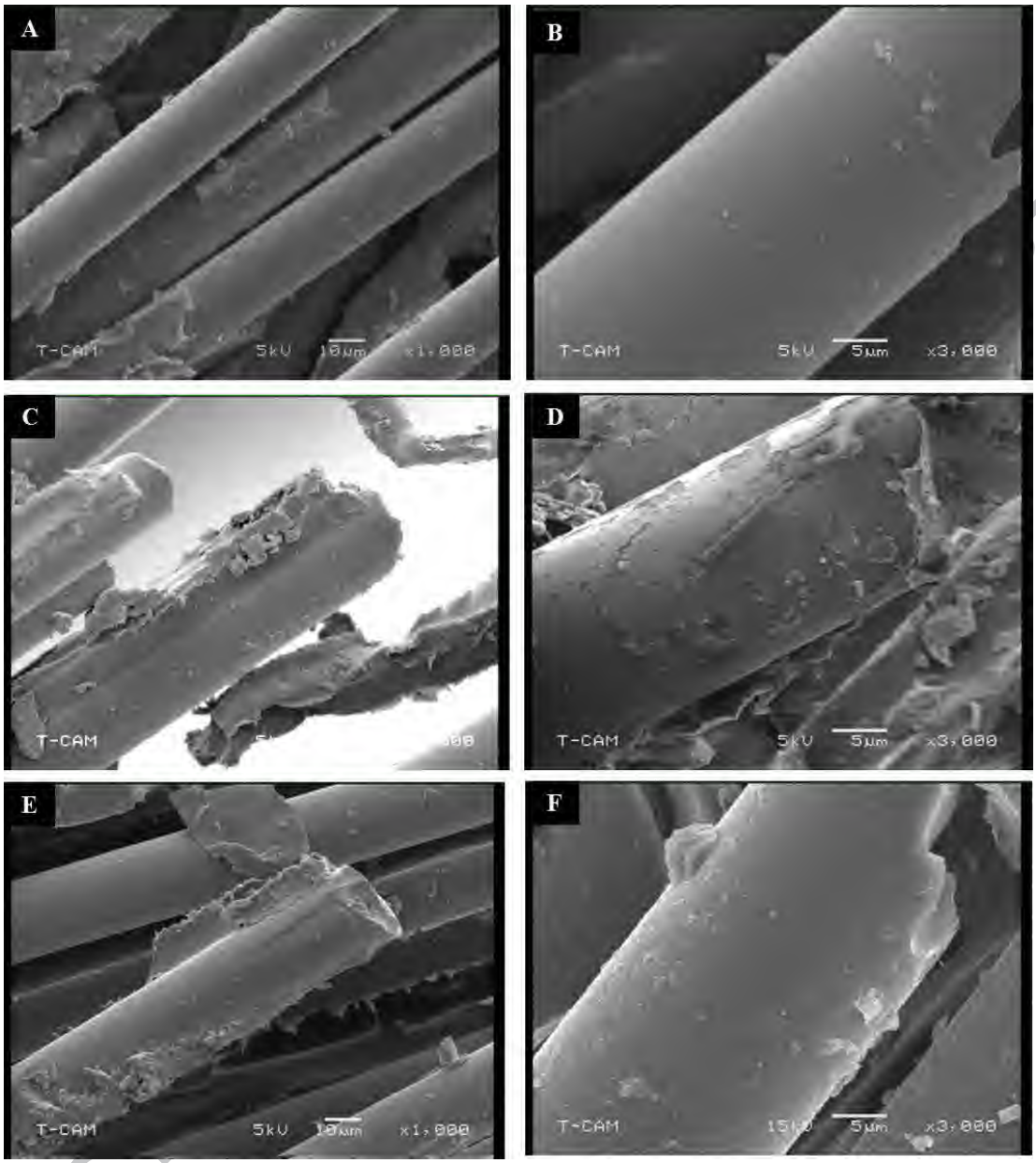

Figure 16 (A-F). SEM micrographs of fractured fiber of A-B) control, C-D) 0.3 wt. % and E-F) 0.4 wt. % MWCNTs e-glass/epoxy composites.

Table 1. Flexural properties of control and MWCNTs epoxy composites.

Specimen	Flexural strain (%)	Flexural Strength (Mpa)	% Change	Flexural modulus (Gpa)	% Change
Control	5.04	83.32±2.7	X	2.4±0.1	X
0.2C	6.09	103.4±0.6	+24	2.69±0.4	+12
0.2S	6.69	107.7±1.8	+29	2.83±0.05	+18
0.3C	6.13	103.7±2.2	+24.5	2.66±0.3	+11
0.3S	7.31	118.5±2.4	+42	2.89±0.1	+20
0.4C	5.83	96.4±0.6	+15.7	2.64±0.1	+10
0.4S	6.21	104.2±1.5	+25	2.77±0.1	+15

Table 2. Flexural properties of control and MWCNTs e-glass/epoxy composites.

Specimen	Flexural strain (%)	Flexural Strength (Mpa)	% Change	Flexural modulus (Gpa)	% Change
Control	1.71	423.7±11.4	X	26.17±1.2	X
0.2C	1.81	486.53±22.3	+15	28.26±0.8	+8
0.2S	2.11	521.3±21	+23	29.33±0.4	+12
0.3C	1.75	506.9±6.5	+19.6	29.77±0.6	+14
0.3S	2.08	513.4±10	+21	31.16±0.9	+19
0.4C	1.78	420.8±27.7	-0.7	27.32±1.5	+4.4
0.4S	1.67	454.4±15.5	+7	29.77±1.8	+14